Journal of Engineering and Sustainable Development
www.jeasd.org
Vol. 20, No.06, November 2016
ISSN 2520-0917

EXPERIMENTAL AND NUMERICAL STUDY OF THE HEAT TRANSFER COEFFICIENTS OF DOUBLE PIPE HELICALLY COILED HEAT EXCHANGER

Ammar A. Hussain[1], Ali S. Golam[2]

1) Assistant Lect., Mechanical Engineering Department, Al-Mustansiriayah University, Baghdad, Iraq.
2) Assistant Lect., Mechanical Engineering Department, Al-Mustansiriayah University, Baghdad, Iraq.

Abstract: This work introduces an experimental and numerical study of the heat transfer coefficients of double pipe helically coiled heat exchanger. It tested for both parallel and counter flow arrangements. Water is used as working fluid in inner tubes side and annulus tube side. The mass flow rate has range between (0.032 - 0.0721) kg/s for cold water while hot water is kept constants at (0.0724 kg/s). Also the range of inlet temperatures of cold and hot water are (20 - 25°C), and (40 - 70 °C), respectively. All experiments performed at the Dean Number for annulus tubes side range of (1250 - 1700). The study directed to focus on influencing the inlet mass flow rate of annulus tubes-side, and inlet temperatures of inner tubes-side over the effectiveness, axial temperature distribution of heat exchanger, efficiency and heat transfer coefficient. All experimental data performed at the steady-state conditions. The results show that the mass flow rate ratio ($\dot{m}_r$) effects the axial temperature distribution of heat exchanger also, the effectiveness and efficiency decreased by increasing mass flow rate ratio. Likewise, comparisons between numerical and experimental results have been made. Empirical correlations between the Nusselt Number with Dean and Prandtl Numbers for the annulus tube have been found.

Keywords*: heat exchanger, Helically Coiled, Double Pipe, Heat Transfer Coefficients*

دراسة عملية وعددية لمعامل انتقال الحرارة لمبادل حراري مكون من ملف حلزوني مزدوج الانبوب

الخلاصة: - يقدم هذا العمل دراسة عملية وعددية لمعامل انتقال الحرارة لمبادل مزدوج الانبوب ملفوف بشكل حلزوني. جرى الاختبار للجريان المتوازي والمتعاكس. تم استعمال الماء كسائل تشغيل من جانب الانبوب الداخلي والحلقي. نسب التدفق تتراوح بين 0.072 (0.032 - kg/s) للماء البارد بينما للماء الحار يبقى ثابت عند (0.0724 kg/s) . مدى درجات الحرارة لدخول الماء البارد والحار تتراوح بين (20 - 25 °C) و (40 - 70 °C) وعلى التوالي. كل الاختبارات اجريت لاعداد دين (D_e) من جانب الانبوب الحلقي تتراوح بين (1250 - 1700). تركز الدراسة على تأثير كل من معدل التدفق للانبوب الحلقي ودرجة الحرارة للانبوب الداخلي على شكل توزيع درجات الحرارة المحوري داخل المبادل، وفعالية وكفاءة المبادل، ومعامل انتقال الحرارة. تظهر النتائج ان لنسبة التدفق ($\dot{m}_r$) تأثير واضح على شكل توزيع درجات الحرارة المحورية للمبادل. وتؤثر زيادتها سلبا على فعالية وكفاءة المبادل. تم مقارنة النتائج العددية والعملية . تم ايجاد معادلة تجريبية لربط عدد نسلت من جانب الانبوب الخارجي بكل من عدد برانتل وعدد دين .

*Corresponding Author ammar.asmf1974 @gmail.com

1. Introduction

Helically coiled tubes heat exchangers are stand out among the most widely recognized hardware found in numerous mechanical applications going from solar energy applications, nuclear power production, chemical and food industries, and other applications. Helical coil is used for transferring heat of chemical reactors because heat transfer coefficients are higher in this type. This is especially important when chemical reactions have high heats of reaction and the heat generated has to be transferred rapidly to maintain the temperature of the reaction. Also, because it has a compact configuration, more heat transfer surface can be given per unit of space than by the use of straight tubes. The shape in the tubes makes a secondary flow, which is normal to the primary axial direction of flow. The secondary flow pattern of the fluid improves the heat transfer rate and the outer fluid moves with a higher velocity compared to the inner fluid due to the effect of curvature ratio. This secondary flow increases the heat transfer between the wall and the streaming fluid. And they offer a greater heat transfer area inside a small space, with greater heat transfer coefficients. The advantage for use double-pipe helical coil is that the flow in the annulus will also experience secondary flows [1]. For decades, many of the helically coiled-tube devices employed for augmentation of laminar or turbulent flow heat transfer have been calculated and discussed.

Rennie [1] studied the double-pipe helical coil heat exchangers experimentally and numerically neglecting the effect of coiled tube pitch. The boundary condition was different from the boundary conditions of constant wall temperature and constant heat flux. In any case, it is clear that the geometry of the double-pipe coiled tube heat exchanger is completely different from that of annulus and inner tube heat exchanger. Both parallel flow and counter flow configuration were studied. Nusselt number in the inner tube was compared to the information got in literature, and Nusselt number in annulus was compared to the numerical results. Nusselt numbers for the annulus were connected with an altered Dean number, resulting in a strong linear relationship as follows:

$$Nu = 0.075De + 5.36 \quad (1)$$

CFD analysis of heat transfer in a helical coil tube using fluent code was investigated by Soumya [2].

The work is an attempt to show the effect of two different flows (parallel and counter) on the total heat transfer from a helical tube. The cold fluid flows in the annulus and the hot fluid flowing in the inner tube of the heat exchanger. Different dimensions of the tubes helix are taken into consideration while running the analysis. Copper was chosen as the metal for development of the helical tube. The governing equations of mass, momentum and heat transfer were solved simultaneously, using the k-*e* two equations turbulence model. Nusselt Number, contours of temperature and energy, velocity vectors and heat transfer rate from the wall of the tube were plotted using ANSYS Fluent 13. The fluid flowing through the tube was taken as water. The study showed that there is not much difference in heat transfer performances for both

the parallel-flow and the counter-flow configuration. Nusselt number at different points along the tubes length was determined from the numerical solution. The numerical simulation was down for water to water heat transfer and different inlet temperatures were studied. A numerical study of helical coil tube-in-tube heat exchanger was studied by Kanungo [3] for different boundary conditions of heat transfer and for different D/d ratio.

The turbulent flow with counter flow heat exchanger is considered for investigation purpose. It was found out that the D/d ratio has effect on heat transfer rate and pumping power. The D/d ratio is differed from 10 to 30 with a step of 5. Nusselt number, friction factor, pumping power and Log mean temperature difference variation of inner fluid with respect to Reynolds Number are carried out for different D/d ratio. The optimum Reynolds number for maximum heat transfer and minimum power loss is calculated by graph intersection methods. The results shown fluid flow behavior is captured for both fluids flowing inside the tube. With expansions in D/d ratio the Nusselt number will decrease and the outer wall boundary condition does not have any effect on the inner Nusselt number. The friction factor decreases with increase in Reynolds number. The Pumping power increases as increase Reynolds number for all D/d ratios and for all boundary conditions. Log mean temperature difference increases with increase in Reynolds number.

ANSYS Fluent studies of heat transfer rate of a tube in tube helical coil heat exchanger were studied by Mohammed et al [4]. An analysis has been done for a tube-in-tube helical coil heat exchanger with constant heat transfer coefficient for turbulent flow. The study is done for different boundary conditions and optimizes condition of heat transfer is found out for various D/d ratio. The turbulent flow model with counter flow heat exchanger is considered for investigation purpose. The effect of D/d ratio on heat transfer and pumping power was found out for different boundary conditions. The study showed that with increase in the Reynolds number, the Nusselt number for the inner tube increases. The increases in flow rate turbulence between the fluid elements will enhance the mixing of the fluid and eventually the Nusselt number. With increases in D/d ratio (inverse of curvature ratio) the Nusselt number will decrease for a particular value of Reynolds number. Nusselt number has maximum quality for D/d=25. The outer wall boundary condition does not have any significant effect on the inner Nusselt number.

Zhang and Li [5] focused on the effect of eccentricity ratios of tube in tube helically heat exchanger by numerical study for turbulent flow under different flow rates. The fluid considered is Helium at pressure of 20Mpa, with temperature dependent thermos physical properties for the inner tube and annulus. The results show that with the eccentricity increasing the annulus Nusselt number increases. According to the numerical data, new empirical correlations of Nusselt number as function of Reynolds Number and eccentricity for the inner and annulus tube was reported. Ritesh et al [6] performed a numerical analysis of heat transfer enhancement in pipe-in-pipe helical coiled heat exchangers. They focused on the effect of the inside tubes at constant value of mass flow rate and variation of annulus mass flow rate on overall heat transfer coefficient and Dean number with constant wall temperature. Additionally deals with

the effect of Dean number with respect to Reynolds number, Nusselt number and overall heat transfer coefficient on change of coil configuration of helically coiled tube. The result was compared with other similar studies in boundary conditions for the helical coils.

They concluded that with the decrease the inner coil diameter, the overall heat transfer coefficient is increased. Ritesh and Kamal [7] determined experimentally the heat transfer enhancement of pipe-in-pipe helical coil heat exchanger.

They focused on experimental investigation into water-to-water heat transfer enhancement of pipe-in-pipe helical coil tubes. Heat transfer characteristics inside pipe-in-pipe helical coils for different boundary conditions, such as constant temperature at hot water inlet, constant mass flow rate are considered.

They concluded the heat transfer rate in counter flow direction is much higher due to large average temperature. In contrast with small coil configuration the overall heat transfer coefficient is slightly high, from large coil configuration.

Nusselt number of inner tube in both coil configurations is to be in the counter flow direction is higher when compared with the parallel flow. Dean Number and curvature ratio in a double-pipe helical heat exchanger were investigated by Tuhid and Seyed [8].

The study focused on the effects of Dean Number and curvature ratio on heat transfer and pressure drop characteristics for laminar flow. Helical copper tubes model is used. The results were compared to the values existed in the open literature and a reasonable agreement was observed.

The study showed that the overall heat transfer coefficient increases by increasing the inner and annulus Dean numbers. For a given annulus Dean number, increasing the inner Dean number results in an inevitable asymptotic overall heat transfer coefficient. The results showed that the high Dean number causes high pressure drops. Mathematical models for overall heat transfer coefficient and inner pressure drop were found out.

It can be stated that expanding curvature ratio enhances the heat transfer and causes low pressure drop. Although there are many works done in a double-pipe helical heat exchanger but , there is few investigations on the influence of the annulus tube mass flow rate, and inlet temperatures of inner tube over the axial temperature distribution of heat exchanger, effectiveness, efficiency and heat transfer coefficient.

2. Double-Pipe Helical Heat Exchanger Geometry

The inner tube and annulus tube heat exchanger is shown in Figure (1). In this figure, D is the diameter of the annulus tube, d is the inner tube diameter, and P is the coil pitch.

The curvature ratio is defined as the coil-to-tube diameter ratio, (d_i / Dc). The specification of heat exchanger is given in Table 1.

Table 1. Geometrical characteristics of the heat exchanger.

Item	***mm***
Coil diameter, tube-center-to-tube-center (D_c)	250
Outside diameter of inner copper tube d_o,	10
Inside diameter of inner copper tube d_i	9.15
Outside diameter of annulus tube D_o,	20
Inside diameter of annulus tube D_i	18
Approximate number of turns in helical coil, N	15
Curvature ratio, d_i/D_c	0.0366
Coil pitch, tube-center-to-tube-center P	30
Heat exchanger height H	500

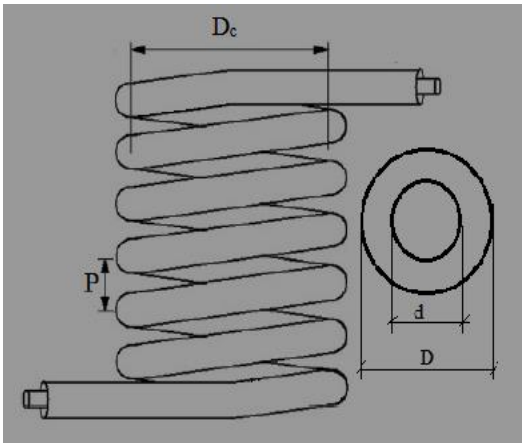

Figure (1) The inner tube and annulus tube heat exchanger

3. Experimental Set Up

Figure (2) shows the schematic diagram of the experimental set-up. It consists of test section and hot and cold water loop. The hot water streams flowing inside the inner tube side while cold water stream flowing in the annulus tube side.

Water was used as the hot and cold fluid. The hot water was pumped to the tank and inner tube, passing through the heater while the cold water was pumped to annulus tube from the tap. The temperature of the inlet hot water to the heat exchanger was controlled by thermostat. Four constant temperatures (50, 60, and 70 °C) were considered for inlet hot water to inner tube. The cold water inlet temperature to annulus tube was the temperature of the tap water.

Temperatures were measured using eight K-type thermocouples placed at equally distanced locations and thermal imager (Ti32). Another four thermocouples were located at inlets and outlets of heat exchanger to measure the temperatures of the hot and cold fluids. Figure (3) shows the apparatus arranged for heat exchanger experiments.

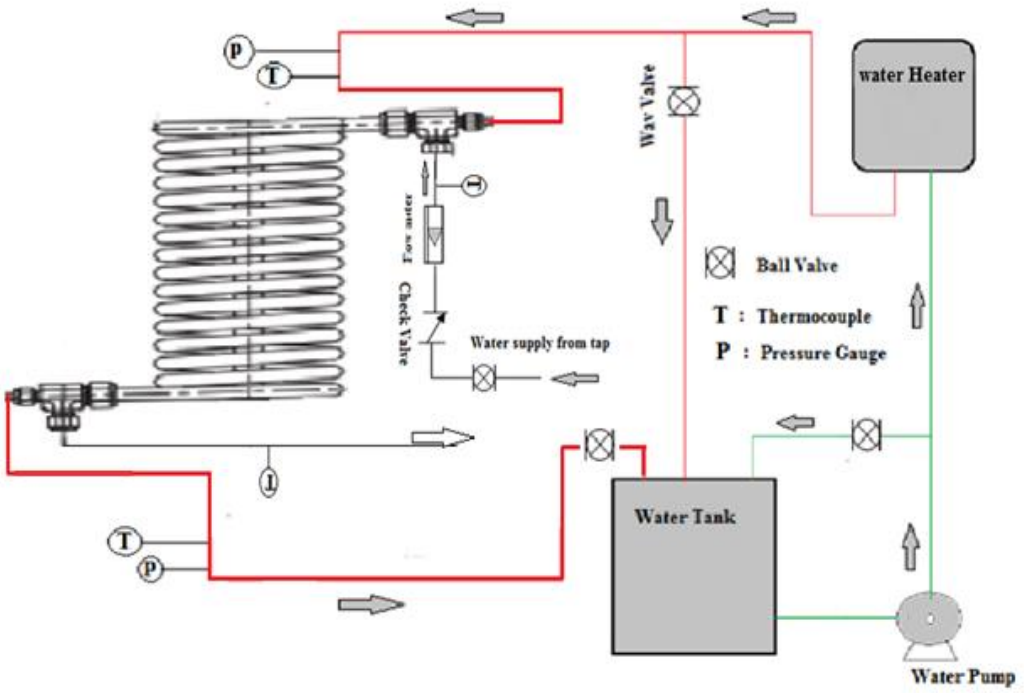

Figure. (2) A schematic diagram of the experimental set-up.

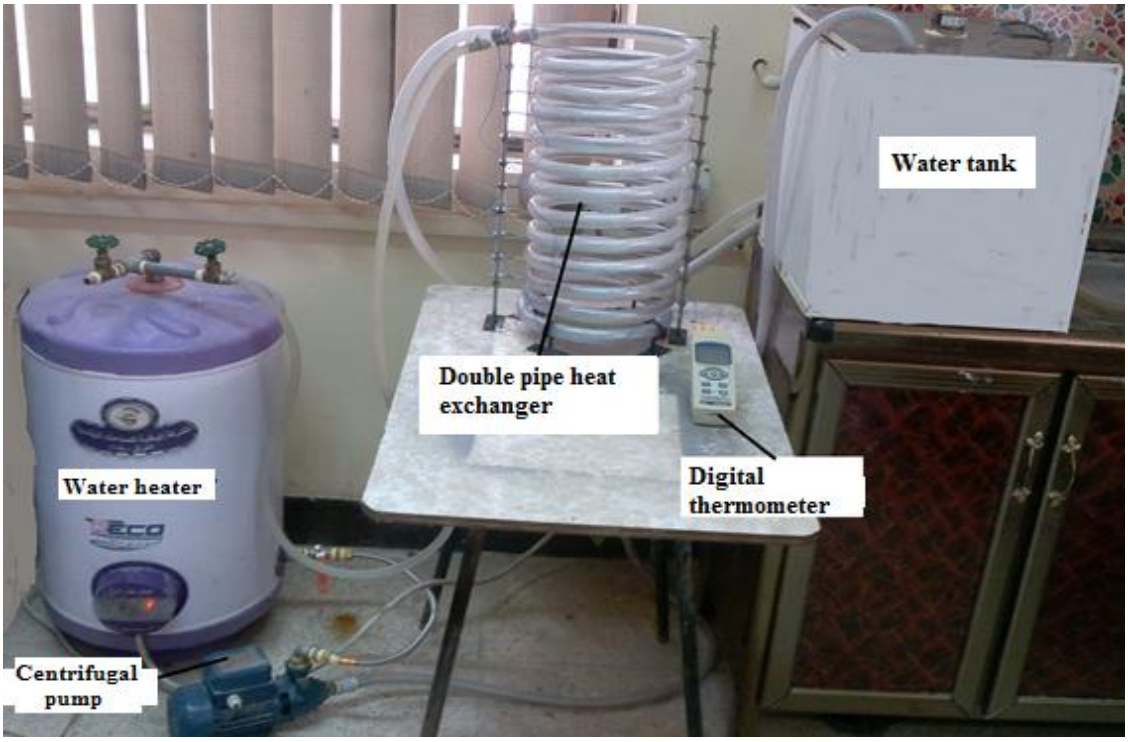

Figure (3) The apparatus arranged for heat exchanger experiments.

4. Basic Equations of Experimental work

Experiments were conducted with different inlet temperatures of hot water and various flow rates of cold water. In the experiments, the system was allowed to approach the steady state. This section describes the methods and basic equations for determining the following parameters on the base of the experimental data:

1) Heat transferred to the hot water in the inner tube, Q_h can be given from by[10]:

$$Q_h = m_h cp_h (T_{hi} - T_{ho}) \quad (2)$$

Where: m_h is the mass flow rate of hot water, cp_h is the specific heat of water, T_{hi} and T_{ho}, are the inlet and outlet hot water temperatures, respectively.

2) Heat transferred from the cold water in the annulus tube, Q_c is given by:

$$Q_c = m_c cp_c (T_{co} - T_{ci}) \quad (3)$$

Where: m_c is the cold water mass flow rate, T_{ci}, and T_{co} are the inlet and outlet cold water temperatures, respectively

3) The average heat transfer rate, Q_{avg}.

$$Q_{avg} = \frac{Q_h + Q_c}{2} \quad (4)$$

In the present study the heat transfer of hot water and the cold water is equal. The energy balance was performed to appraise the degree of any heat losses or gains from the surrounding. Now for minimum error the heat transfer was obtained from Equation (4).

4) The inner tube-side heat transfer coefficient, hi is obtained from Q_{avg}.

$$Q_{(avg)} = h_i A_i (T_{c,s(avg)} - T_{w,h(avg)}) \quad (5)$$

Where: $T_{c,s(avg)}$ is the average inner tube surface temperature given by:

$$T_{c,s(avg)} = \frac{(T_1 + T_2 + \cdots + T_n)}{n} \quad (6)$$

$T_{w,h(avg)}$ is the mean hot water temperature and is given by:

$$T_{w,h(avg)} = \frac{T_{hi} + T_{ho}}{2} \quad (7)$$

A_i is the inside surface area of the inner tube.

,

5) The overall heat transfer coefficient (U)

The overall heat transfer coefficient can be determined from **[10]**:

$$U \cdot A \cdot F = \frac{Q_{avg}}{LMTD} \tag{8}$$

Where: *LMTD*the logarithmic-mean temperature difference and F is the correction factor which is equal to 1 for this case [10].

$$LMTD = \frac{\Delta T_1 - \Delta T_2}{In\left(\frac{\Delta T_1}{\Delta T_2}\right)} \tag{9}$$

Where:

$\Delta T_1 = T_{h,in} - T_{c,in}$
$\Delta T_2 = T_{h,out} - T_{c,out}$ } For parallel flow

$\Delta T_1 = T_{h,in} - T_{c,out}$
$\Delta T_2 = T_{h,out} - T_{c,in}$ } For counter flow

$$Q_{avg} = \frac{LMTD}{R_{total}} = UA\ LMTD = U_i A_i LMTD = U_o A_o LMTD \tag{10}$$

$$\frac{1}{UA} = \frac{1}{U_i A_i} = \frac{1}{U_o A_o} = \Sigma R = \frac{1}{h_i A_i} + R_{wall} + \frac{1}{h_o A_o} \tag{11}$$

6) Nusselt numbers (Nu)

Nusselt number can calculate as**[10]**:

$$Nu_A = \frac{h_o D_h}{k} \tag{12}$$

Where: Nu_A the Nusselt number for annulus tube, D_h, Hydraulic diameter for annulus *tube*, k = Thermal conductivity

7) Reynolds Number (Re) **[10]**:

$$\text{Re} = \frac{VD}{\nu} = \frac{4m^{\bullet}}{\pi D \mu} \tag{13}$$

The Critical Reynolds number according to the research of **Ghorbani [9]** for the helical tube flow, which decides the flow is laminar or turbulent, is related to the curvature ratio as follows**[1]**:-

$$\mathbf{R_{ecrit} = 2100\ [1+ 12(di / Dc)^{0.5}]} \tag{14}$$

8) Dean Number (D_e)

D_e, is a dimensionless group in fluid mechanics, which occurs in the investigation of flow in curved tube, and is defined as**[1]**:

$$D_e=R_e \sqrt{\left(\frac{D_t}{D_c}\right)} \quad (15)$$

9. Heat exchanger effectiveness:

Effectiveness can be defined as the ratio of actual to maximum heat transfer of the heat exchanger. Thermodynamically limited maximum possible heat transfer rate as would be realized in counter flow heat exchanger of infinite heat transfer area this means that**[10]**:

$$\varepsilon = \frac{Q_{act}}{Q_{\max}} \quad (16)$$

where

$$Q_{max} = C_{min}\,(T_{h,i} - T_{c,i}) \quad (17)$$

and C_{min} = ($\dot{m}Cp$) is the minimum heat capacity of cold or hot fluid.

10) Heat exchanger efficiency ξ

The heat exchanger efficiency is defined as the ratio of the actual rate of heat transfer in the heat exchanger to the optimum rate of heat transfer [10]:-

$$\xi = \frac{Q_{act}}{Q_{opt}} \quad (18)$$

where

$\xi = \frac{T_{hi}-T_{ho}}{T_{hi}-T_{ci}}$ For parallel flow, and (19)

$\xi = \frac{T_{hi}-T_{ho}}{T_{hi}-T_{co}}$ For counter flow (20)

5. Numerical Simulation

Generally, numerical simulation required to simulate the interaction of fluids with surfaces by limit boundary conditions, and initial conditions for the case. The double pipe helical coil heat exchanges with turbulent forced convection heat transfer, for different mass flow rate ratio and different temperature inlet are finished by the ANSYS Fluent 14.0 package. The aim at using CFD simulation software is to predict the systems performance. Continuity equation, and energy equation and the Navier Stokes momentum equations govern the flow of the fluid in the helical coil tubes are to be solved. However, the basis of all CFD problems is the Navier stokes equations. In this

section the physical and the computational model are presented in detail. Three dimensions (X, Y, Z) of the double pipe helical coil have been drawn by Solid Work software 2012 and meshed using Gambit geometric modeling software. Also, the model used the tetrahedron mesh. The optimum grid size of the mesh has been choosing by testing different grid size. The simulation software step is shown in figure (4).

- **Boundary conditions**

The conditions of the inlet and outlet of test sections as inlet mass flow rate inlet, temperature, and pressure outlet for both counter and parallel flow of inner tube and annulus tube are prescribed. Copper was taken as the base metal for inner tube due to the high value of thermal conductivity for copper. The details about all boundary conditions are shown in Table (2). The conditions of the side wall of the annulus tube were taken q= 0 W/m^2, because there is no heat transfer takes place from this side of the exchanger. The properties of the working fluid were assumed to be constant throughout the CFD simulation shown in Table (3). Also, the properties of copper tube for the heat exchanger were remains constants throughout the analysis see Table (4).

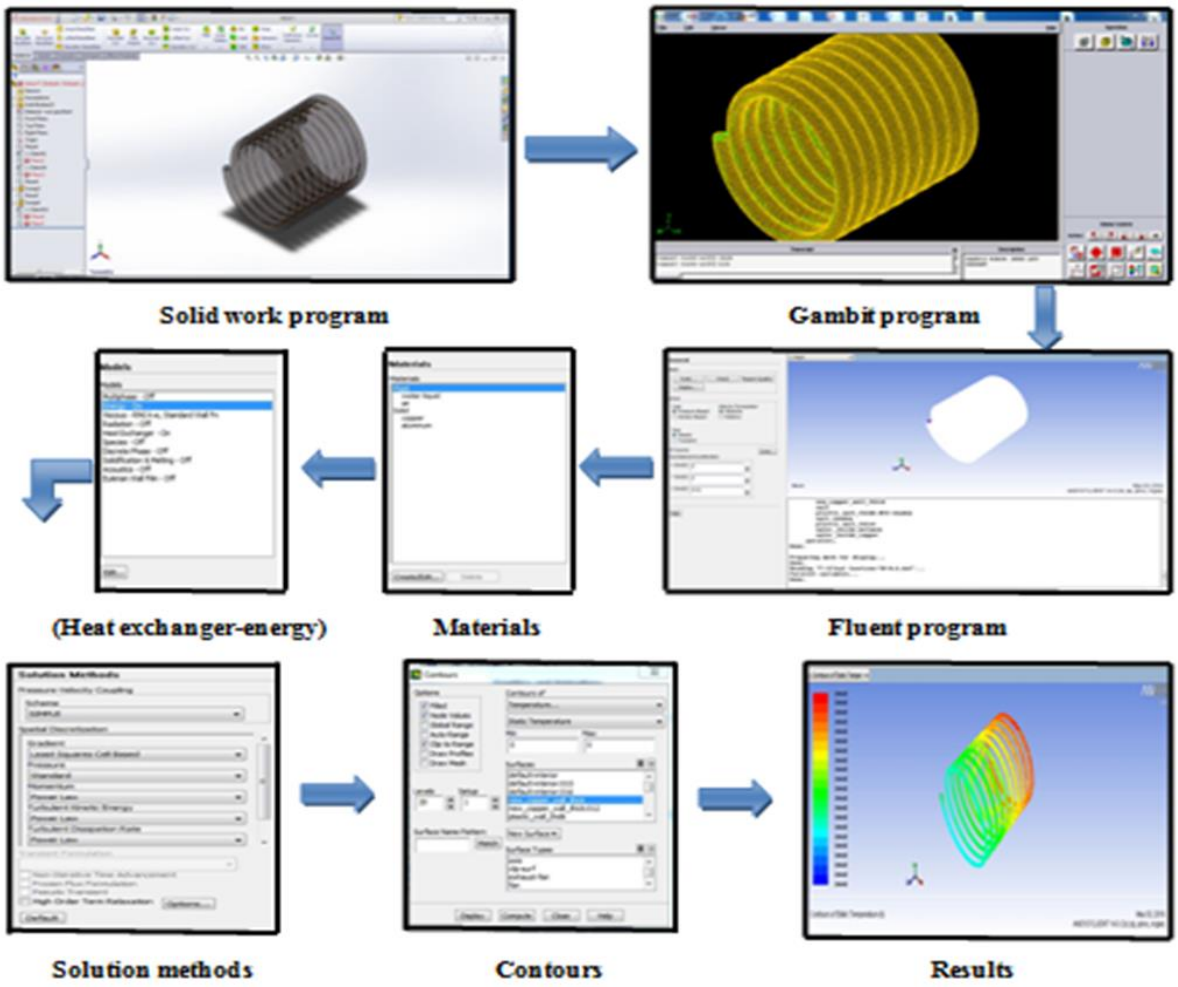

Figure (4) For numerical analysis steps.

Table (2) The details of boundary conditions .

	Boundary condition type	Mass flow rate magnitude kg/s	Turbulent kinetic energy	Turbulent dissipation rate	Temperature °C
Hot water inlet	Mass flow rate Inlet	(0.032,0.048,0.073)	0.01	0.1	(50,60,70)
Cold water inlet	Mass flow rate	0.0724	0.01	0.1	22

Table (3) Properties of water.

Description	value
Viscosity	0.001003 kg/m-s
Density	998.2 kg/m^3
Specific heat capacity	4182 J/kg-K
Thermal conductivity	0.6 W/m-K

Table (4) Properties of copper tube.

Description	value
Density	8978 kg/m^3
Specific heat capacity	381 J/kg-K
Thermal conductivity	387.6 W/m-K

- **Basic assumptions:**

a) Outer wall thickness is neglected to simplify the numerical solution.
b) Steady state heat transfer conditions were assumed.
c) Constant fluid property with incompressible fluid.
d) Natural convention and Radiation was neglected.
e) Conjugate heat transfer between the two fluids was considered.

- **Governing equations**:

The differential governing equation for the fluid flow is given by continuity or mass conservation equation, Navier Stokes equations or momentum conservation equation and energy equation.

1) Continuity equation:

$$\frac{\partial(\rho u)}{\partial x}+\frac{\partial(\rho v)}{\partial y}+\frac{\partial(\rho w)}{\partial z}=0 \tag{21}$$

2) Navier Stokes equation:

$$\rho\left(u\frac{\partial(\rho u)}{\partial x}+v\frac{\partial(\rho u)}{\partial y}+w\frac{\partial(\rho u)}{\partial z}\right)=\rho x+\frac{\partial p}{\partial x}+\frac{1}{3}\mu\frac{\partial}{\partial x}\left(\frac{\partial u}{\partial x}+\frac{\partial v}{\partial y}+\frac{\partial w}{\partial z}\right)+\mu\nabla^2 u \tag{22}$$

$$\rho\left(u\frac{\partial(\rho v)}{\partial x}+v\frac{\partial(\rho v)}{\partial y}+w\frac{\partial(\rho v)}{\partial z}\right)=\rho y+\frac{\partial p}{\partial y}+\frac{1}{3}\mu\frac{\partial}{\partial y}\left(\frac{\partial u}{\partial x}+\frac{\partial v}{\partial y}+\frac{\partial w}{\partial z}\right)+\mu\nabla^2 v \tag{23}$$

$$\rho\left(u\frac{\partial(\rho w)}{\partial x}+v\frac{\partial(\rho w)}{\partial y}+w\frac{\partial(\rho w)}{\partial z}\right)=\rho z+\frac{\partial p}{\partial z}+\frac{1}{3}\mu\frac{\partial}{\partial z}\left(\frac{\partial u}{\partial x}+\frac{\partial v}{\partial y}+\frac{\partial w}{\partial z}\right)+\mu\nabla^2 w \quad (24)$$

3) Energy equation:

$$\rho c_p\left(u\frac{\partial T}{\partial x}+v\frac{\partial T}{\partial y}+w\frac{\partial T}{\partial z}\right)=\left(u\frac{\partial p}{\partial x}+v\frac{\partial p}{\partial y}+w\frac{\partial p}{\partial z}\right)+k\nabla^2 T+\mu\emptyset \quad (25)$$

Where:

$$\emptyset=2\left[\left(\frac{\partial u}{\partial x}\right)^2+\left(\frac{\partial v}{\partial y}\right)^2+\left(\frac{\partial w}{\partial z}\right)^2\right]+\left[\left(\frac{\partial u}{\partial y}+\frac{\partial v}{\partial x}\right)^2+\left(\frac{\partial v}{\partial z}+\frac{\partial w}{\partial y}\right)^2+\left(\frac{\partial w}{\partial x}+\frac{\partial u}{\partial z}\right)^2\right]-\frac{2}{3}\left[\frac{\partial u}{\partial x}+\frac{\partial v}{\partial y}+\frac{\partial w}{\partial z}\right]^2 \quad (26)$$

6. Results and Discussions.

- **Experimental Results:**

Results of the effect of the mass flow rate of inner tube-side to annulus tube-side ratio ($\dot{m_r}$) on the axial temperature profiles of heat exchanger for both parallel-flow and counter-flow is shown in Figure (5) to (10). In all graphs of the axial temperature profile, the one value of the abscissa corresponds to the bottom of the exchanger whereas the value of zero indicates the top. Such that the profiles tend to be concave up, which means that the coil surface temperature is higher than usual at the top and after that it drops faster than usual while moving towards the bottom of the heat exchanger. Figures (5) to (7) show typical temperature distributions inside the heat exchanger for fixed inlet conditions Th,i= 70°C and parallel flow. Figures (8) to (10) show typical temperature distributions inside the heat exchanger for fixed inlet conditions Th,i = 70°C and counter flow. It can be seen that the temperature rise of cold fluid is equal to the temperature drop of the hot fluid that means axial temperature profile of the coil surface is close to from being linear for those figures. The mass flow rate ratio has little effect on the typical temperature distributions of the heat exchanger.

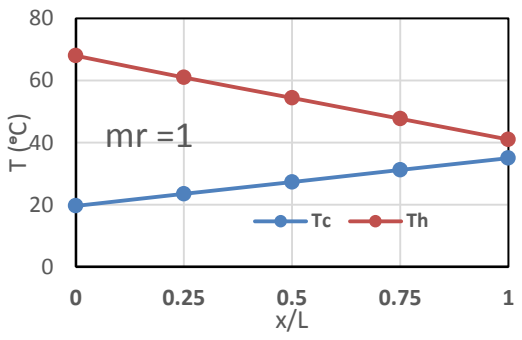

Fig.(5) Temperature distribution for m_r = 1 (parallel flow)

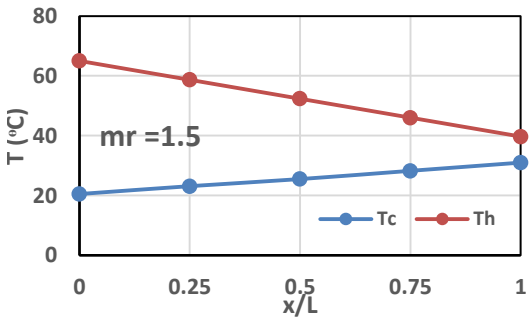

Fig.(6) Temperature distribution for mr = 1.5 (parallel flow)

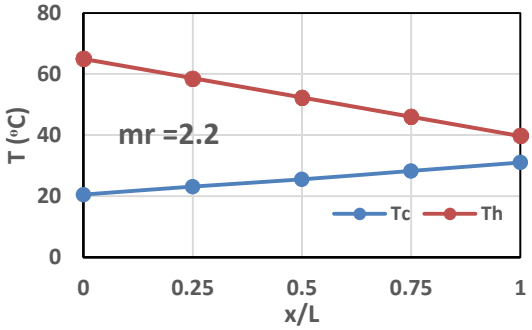

Fig.(7) Temperature distribution for m_r =2.2 (parallel flow)

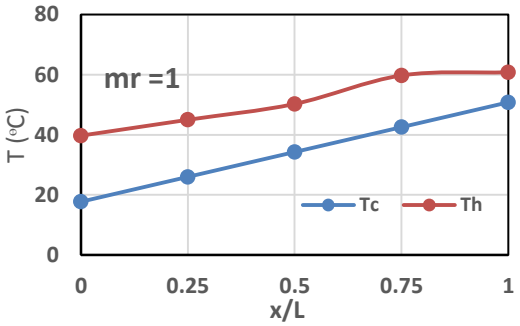

Fig.(8) Temperature distribution for m_r = 1 (counter flow)

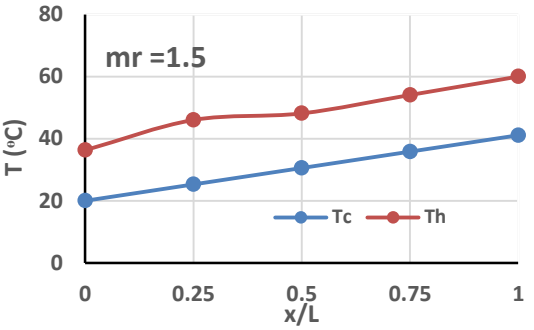

Fig.(9) Temperature distribution for m_r =1.5 (counter flow)

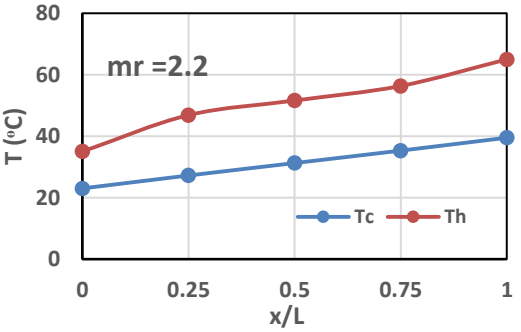

Fig.(10) Temperature distribution for m_r = 2.2 (counter flow)

Figure (11), (12) shows typical relationship between the inlet hot temperature with heat transfer rates and *LMTD*. This is evident from these figures that are representing the typical behavior of LMTD. It can be seen the effect of increased heat rate on the value of LMTD.

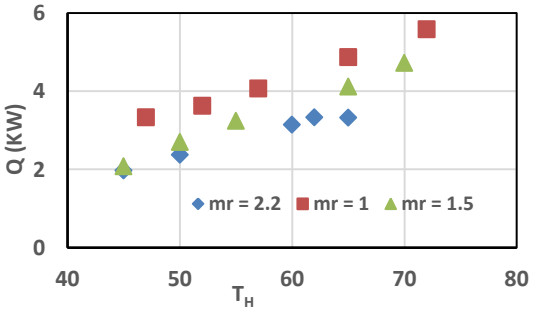

Fig. (11) Heat transfer rates versus inlet hot temperature

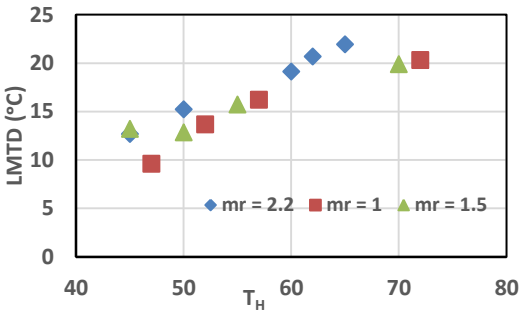

Fig. (12) LMTD versus inlet hot temperature

Figure (13) shows the relation between the heat transfer rates with mass flow rate ratio for both parallel-flow and counter-flow configurations. The heat transfer rates are highly dependent on decreasing the thermal resistance of the coiled tube. Physically, increasing mass flow rate is translated into a decreasing in the value of the heat transfer. This figure show that the heat load of the counter flow is higher than the heat load of the parallel flow. Also a heat transfer rate of the counter flow is higher than parallel flow

due to increase of the *LMTD*. The figure also show that the overall heat transfer coefficient for both parallel-flow and counter-flow configurations is increasing when the heat load increasing. Physically, the overall heat transfer coefficient increases as a result of the thermal resistance decreased.

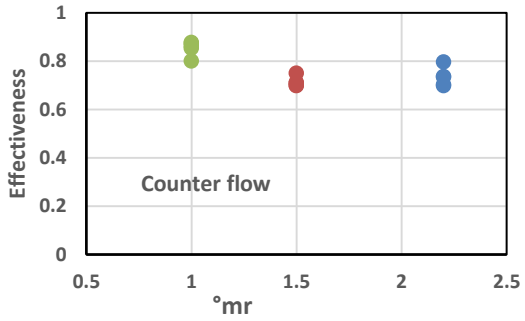

Fig. (13) Heat transfer rates versus inlet hot temperature

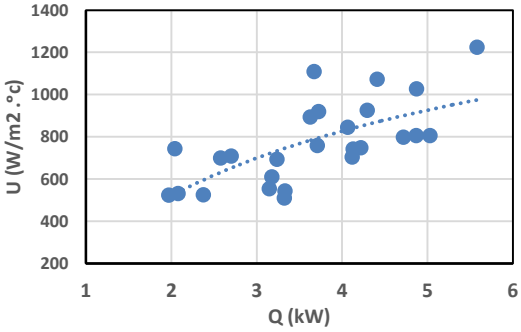

Fig.(14)The overall heat transfer coefficient versus heat rate

Results of the effect of the mass flow rate ratio on the effectiveness are shown in Figs (15) and (16) for both counter and parallel flow configurations. It can be seen in these figures the slope of the curve decreased as the value of the mass flow rate increased. Physically, increasing the mass flow rate ratio leads to an increase in the thermal resistance which translates into a decrease in the value of the heat transfer. Also, an effectiveness of the counter flow is higher than parallel flow due to increase of the heat load.

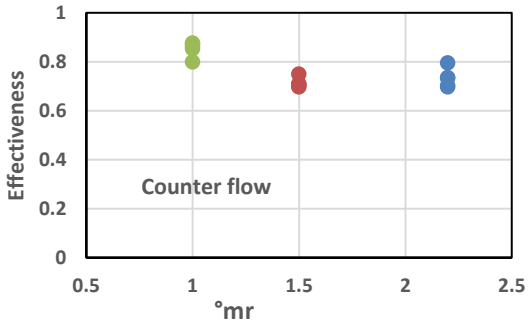

Fig.(15) Effectiveness versus $°m_r$ for counter flow

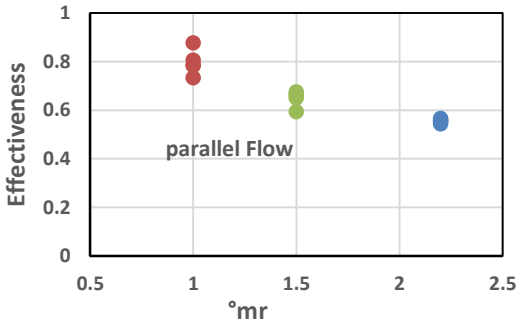

Fig.(16) Effectiveness versus m_r for parallel flo

Results of the effect of the mass flow rate ratio on the efficiency are shown in Fig (17) for both parallel and counter flow configurations. It can be seen in these figures the slope of the curve decrease as the value of the mass flow rate increases. Physically, increasing the mass flow rate ratio leads to an increase in the thermal resistance which translates into a decrease in the value of the heat transfer. Also an efficiency of the counter flow is higher than parallel flow due to increase in the heat load. Fig. (18) show the plot of the Nusselt and Prandtl numbers based on the experimental results against the Dean number *(R^2 = 0.94)* for this graph. The correlation between the current

experiment data obtained from the curve fitting for the range of ($1< \dot{m}_r < 2.2$), (1250< De < 1700) is as follow:

$$Nu_h = 1.964\times10^{-6} De^{2.2392} P_r^{0.3} \quad (27)$$

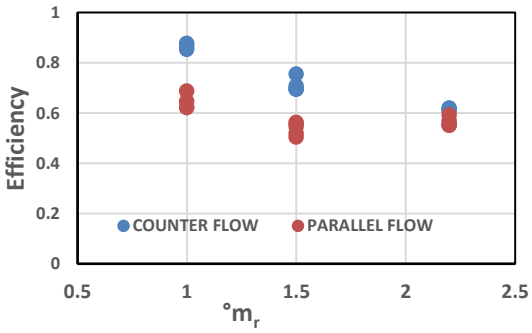

Fig.(17) Efficiency versus $°m_r$

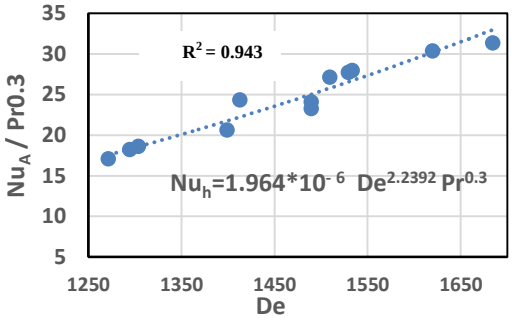

Fig.(18) $Nu_A / Pr^{0.3}$ versus the Dean number

- **Numerical Result**

Figures (19) and (20) show comparison between the numerical results of ANSYS with photos of thermal cameras for temperature distributions inside the heat exchanger. This results for boundaries condition (T_h =70 °C, $\dot{m}_r$=1, and counter flow) show that the simulation data are in good agreement. The numerical results for temperature distribution across the length has been estimated as shown in figures (21) to (29) temperature contours of heat exchanger for both parallel and counter flow configurations with different hot temperate and different mass flow ratio. For all figure that the coil surface temperature is higher than at the top and then it drops faster than moving towards the bottom of the heat exchanger for parallel flow while for the counter flow is reversing. Figure (21) show the temperature contours of heat exchanger for both parallel and counter flow at m_r = 2.2 and $T_{h,i}$ = 50°c. Figure (22) show the temperature contours of heat exchanger for both parallel and counter flow at m_r = 2.2 and $T_{h,i}$ = 60°c. Figure (23) show the temperature contours of heat exchanger for both parallel and counter flow at m_r = 2.2 and $T_{h,i}$ = 70°c. Figure (24) show the temperature contours of heat exchanger for both parallel and counter flow at m_r = 1.5 and $T_{h,i}$ = 50°c. Figure (25) show the temperature contours of heat exchanger for both parallel and counter flow at m_r = 1.5 and $T_{h,i}$ = 60°c. Figure (26) show the temperature contours of heat exchanger for both parallel and counter flow at m_r = 1.5 and $T_{h,i}$ = 70°c. Figure (27) show the temperature contours of heat exchanger for both parallel and counter flow at m_r = 1 and $T_{h,i}$ = 50°c. Figure (28) show the temperature contours of heat exchanger for both parallel and counter flow at m_r = 1 and $T_{h,i}$ = 60°c. Figure (29) show the temperature contours of heat exchanger for both parallel and counter flow at m_r = 1 and $T_{h,i}$ = 70°c. The numerical results of all figure show that the temperate drop in heat exchanger is higher than at the m_r = 2.2 and $T_{h,i}$ = 70°c for both parallel and counter flow with comparing with different situations above.

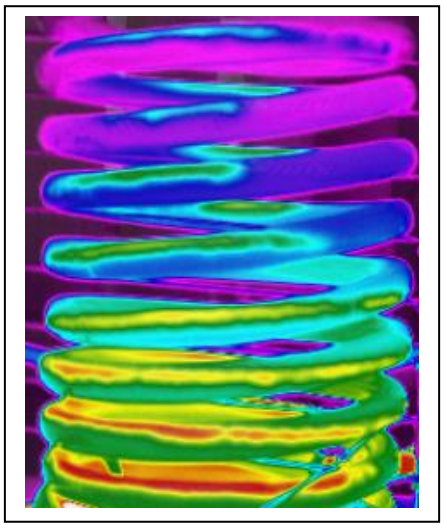

Fig. (19) Photos of thermal camera

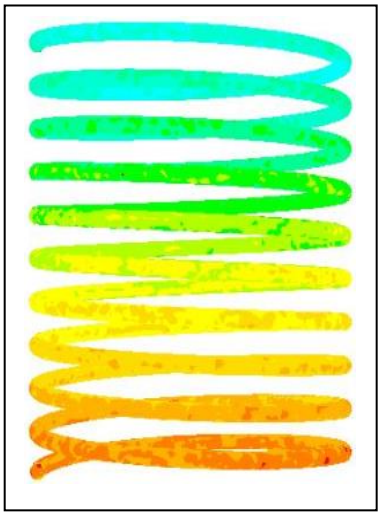

Fig.(20) The numerical results

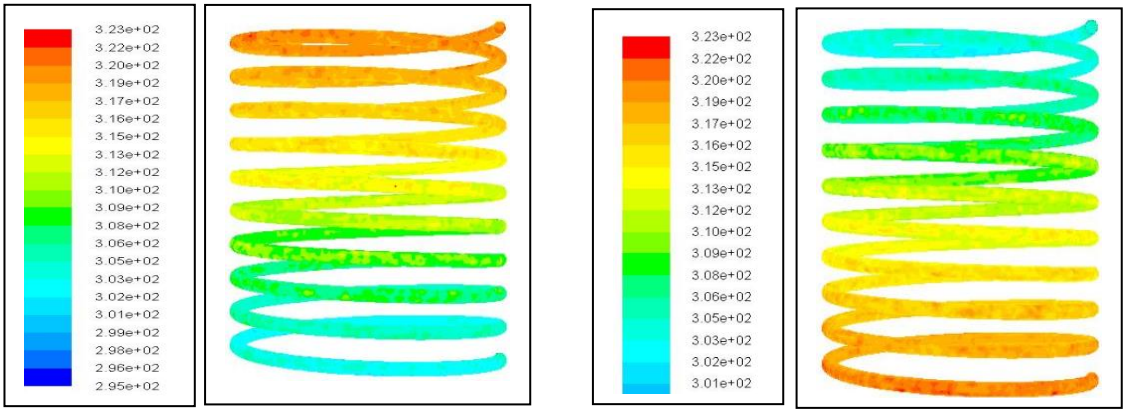

Fig. (21) Temperature contours of heat exchanger for both parallel flow and counter flow at m_r =2.2 and T_h= 50ºc

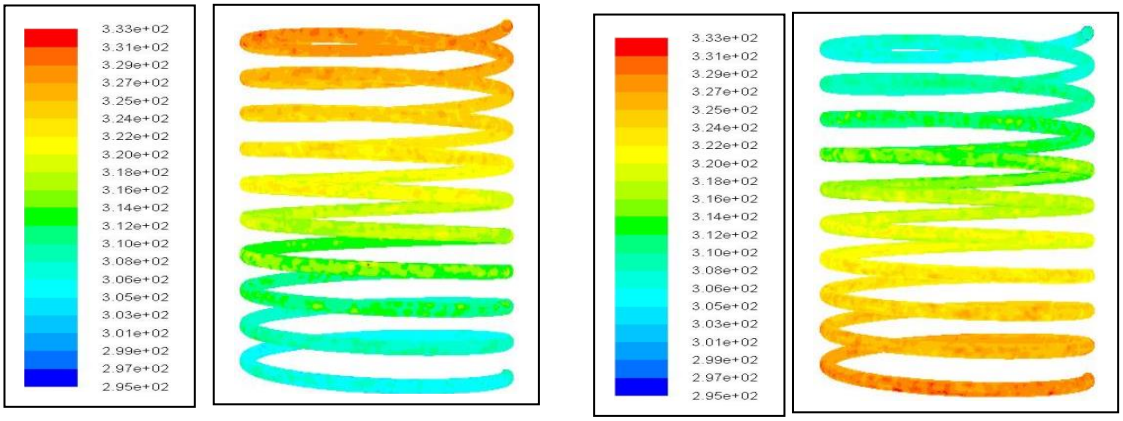

Fig. (22) Temperature contours of heat exchanger for both parallel flow and counter flow at m_r =2.2 and T_h= 60ºc

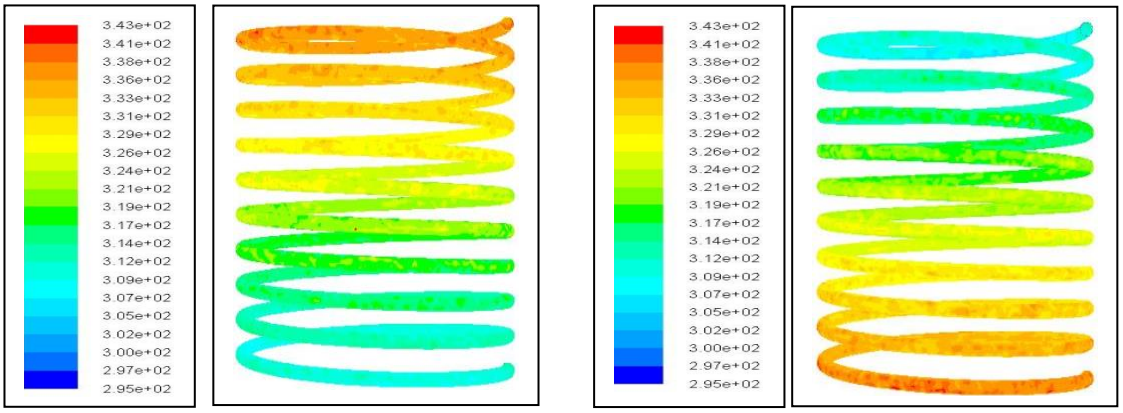

Fig. (23) Temperature contours of heat exchanger for both parallel and counter flow at m_r =2.2 and T_h= 70ºc

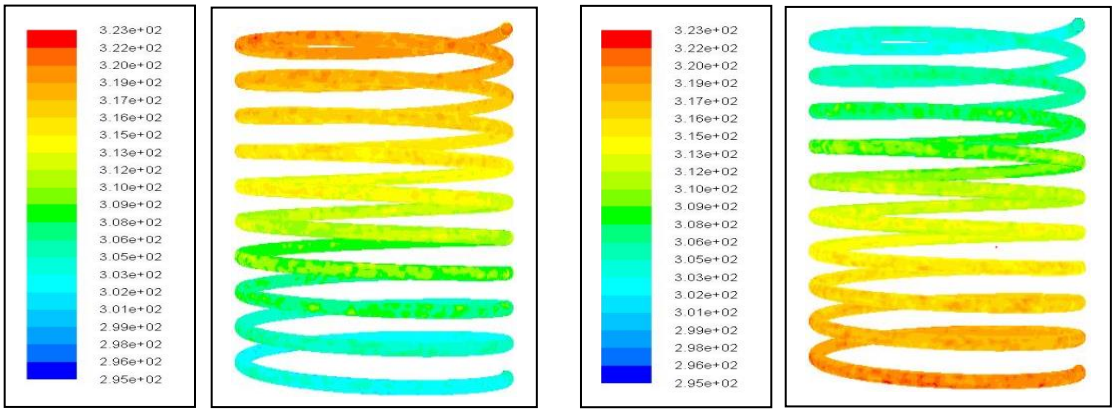

Fig. (24) Temperature contours of heat exchanger for both parallel and counter flow at m_r =1.5 and T_h= 50ºc

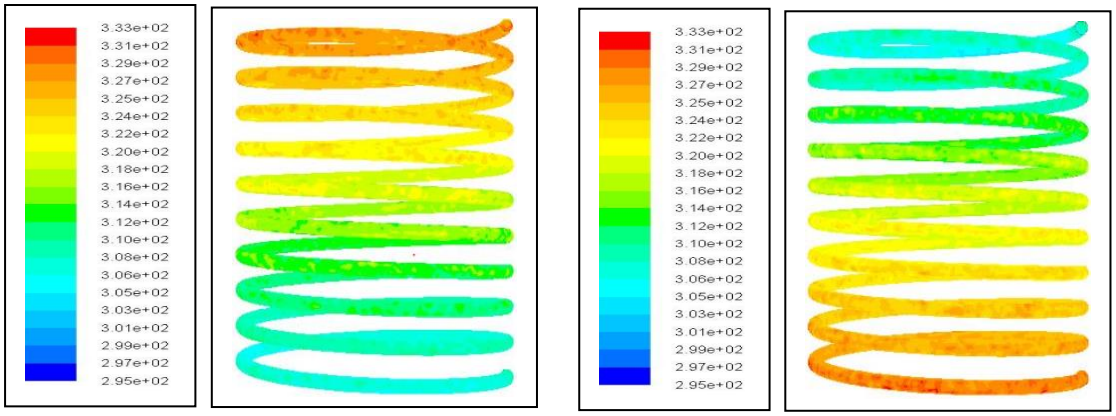

Fig. (25) Temperature contours of heat exchanger for both parallel and counter flow at m_r =1.5 and T_h= 60ºc

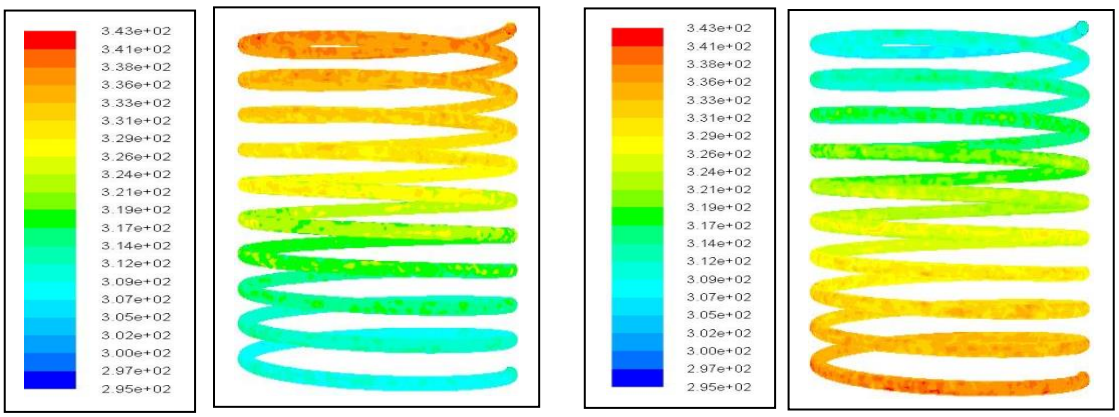

Fig. (26) Temperature contours of heat exchanger for both parallel and counter flow at m_r =1.5 and T_h= 70ºc

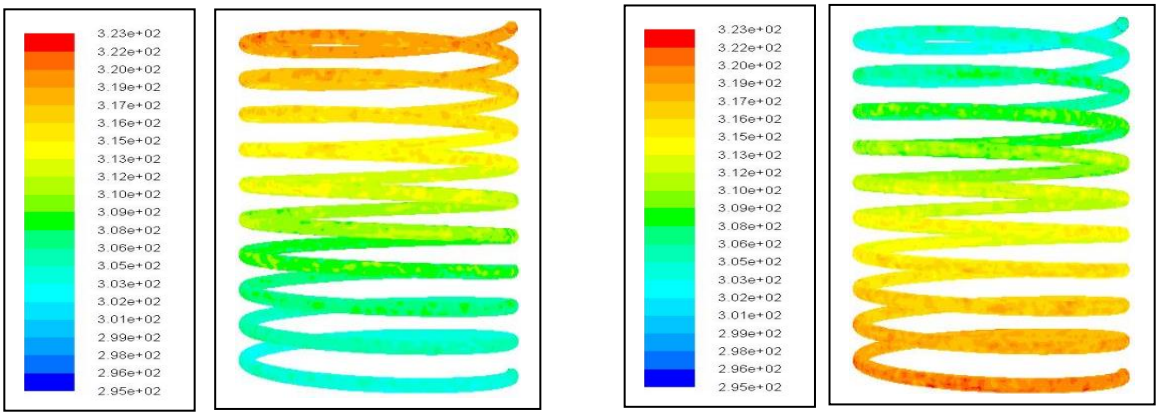

Fig. (27) Temperature contours of heat exchanger for both parallel and counter flow at m_r =1 and T_h= 50ºc

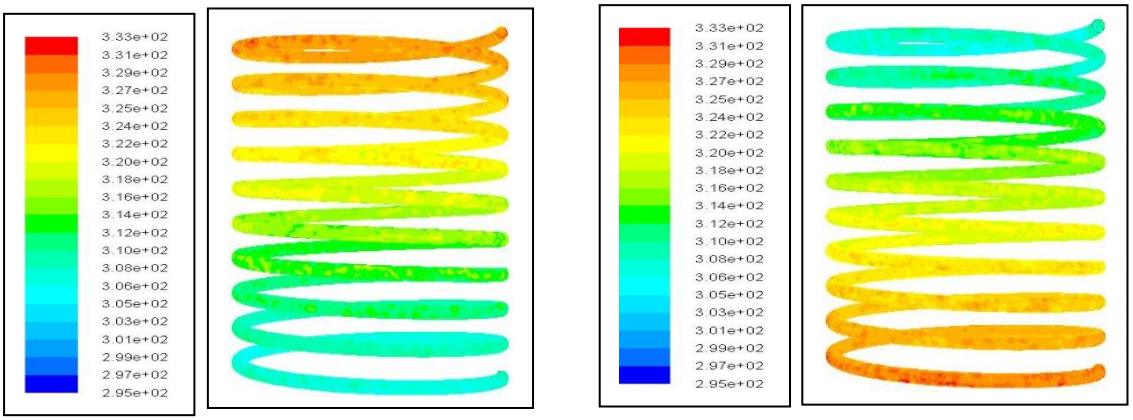

Fig. (28**)** Temperature contours of heat exchanger for both parallel and counter flow at m_r =1 and T_h= 60ºc

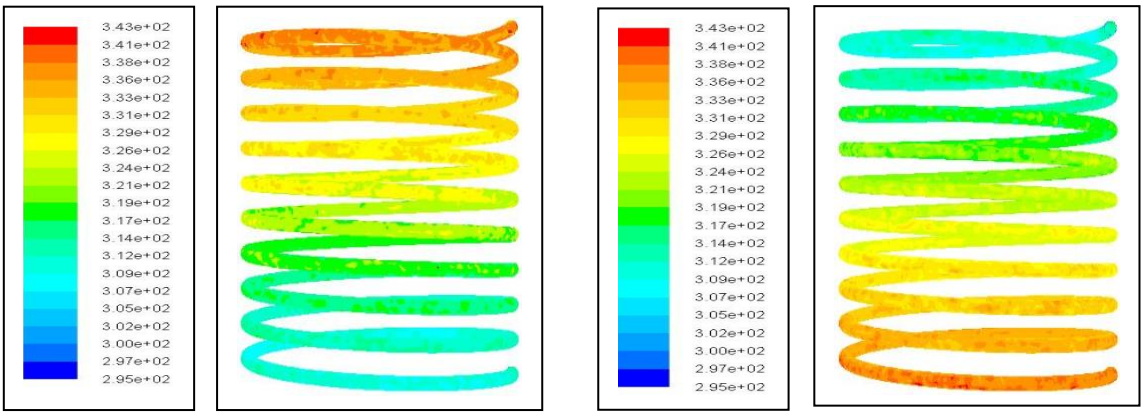

Fig. (29) Temperature contours of heat exchanger for both parallel and counter flow at m_r =1 and T_h= 70°c

- **Validation of Numerical Simulation**

In order to validate our numerical simulation, a comparison has been carried out with numerical and experimental results. The results of numerical simulation were recorded for the locations more than considered in the experimental. Numerical and experimental results of the effect of the mass flow rate of inner tube-side to annulus tube-side ratio ($\dot{m_r}$) on the axial temperature profiles of heat exchanger for fixed inlet conditions (Th,i = 70°C, $\dot{m_r}$= 2.2 and counter flow) is shown in figure (30). Agreement between the numerical and experimental data is fairly good and percentage of difference between the experimental and numerical is 5% in this figure.

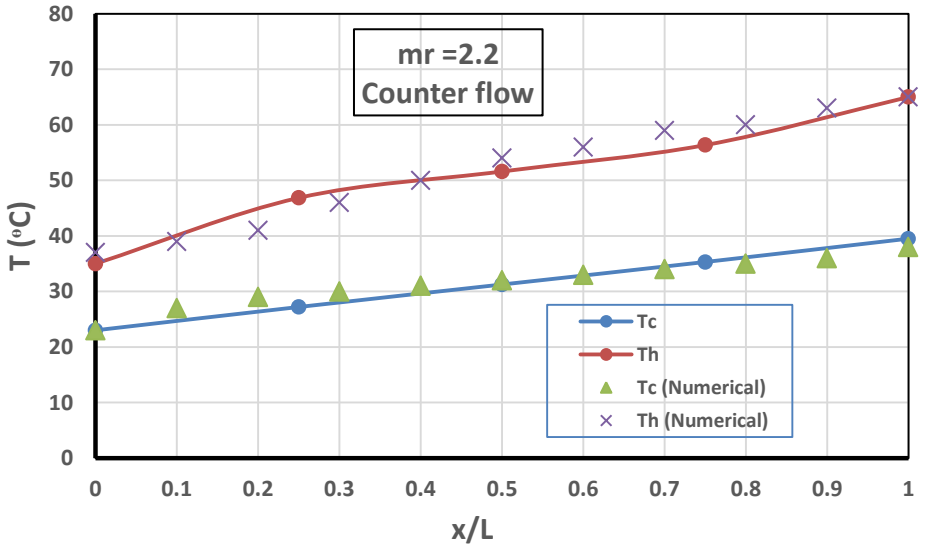

Figure (30) numerical and experimental results for the axial temperature profiles of heat exchanger.

7. Conclusions

In present work, an experimental and numerical investigation into the convection heat transfer in a vertical helically coiled double pipe heat exchanger was carried out. The study has the following conclusions:

- The mass flow rate of inner tube side to annulus tube side ratio (m_r) was found to be effective parameter on the axial temperature distribution of heat exchanger.
- The effectiveness and efficiency of heat exchanger decreased with increasing mass flow rate ratio for both parallel and counter flow configuration.
- The efficiency and effectiveness of the counter flow is higher than parallel flow.
- The inlet hot water temperature showed a positive effect on both *LMDT* and heat transfer rates.
- The overall heat transfer coefficient of heat exchanger increases with increasing the heat transfer rate.
- The correlation between the Nusselt number and Dean and Prandtl numbers could be obtained.

Nomenclature

Symbol	*Description*	*Units*
A	Tube cross-sectional area	m^2
A_c	surface of the coiled tube	m^2
Cp	Specific heat	J/kg. K
D, d	Diameter, for annulus and inner tube	m
D_h	Hydraulic diameter for annulus tube	m
De	Dean number	---
H	Heat exchanger height	m
h	Heat transfer coefficient	$(W/m^2 \cdot K)$
k	Thermal conductivity	$(W/m \cdot K)$
L_c	Total length of coils	m
LMTD	Logarithmic mean temperature difference	^oC
$\dot{m}$	Mass flow rate	kg/s
$\dot{m}_r$	Inner tube-side to annulus tube-side mass flow rate ratio	---
N	Number of coils turns	---
Nu	Nusselt number	---
P	Coil pitch	mm
Pr	Prandtl number,	---
Q	Heat transfer rate	Watt
Re	Reynolds number ,	---
R^2	Correlation Coefficient	---
T	Temperature	^oC
U	Overall heat transfer coefficient	$W/m^{2.} K$

Greek Symbols	*Description*	*Units*
ΔT	Temperature difference	^{o}C
μ	Fluid viscosity	kg/m.s
ρ	Mass density	kg/m^3
υ	Kinematic viscosity	m^2/s
ε	Heat exchanger effectiveness	-------
ξ	Heat exchanger efficiency	-------

Subscripts	*Description*
c	Cold water
h	Hot water
i	Inner
o	Outer
r	Ratio
act	Actual
opt	Optimum
s	Surface

8. Reference

1. T.J. Rennie, (2004), Numerical and experimental studies of a double-pipe helical heat exchanger, Ph.D. Thesis, McGill University, Montreal, Canada.

2. S. R. Mohanty, (2013), "CFD analysis of heat transfers in a helical coil heat exchanger using fluent "B.SC. Project, Department of Mechanical Engineering National Institute of Technology.

3. S. Kanungo, (2014)," Numerical analysis to optimize the heat transfer rate of tube-in-tube helical coil heat exchanger " M.Sc. Thesis, Department of Mechanical Engineering National Institute of Technology.

4. M. Imran, G. Tiwari and A. S. Yadav, (2015)," CFD Analysis of Heat Transfer Rate in Tube in Tube Helical Coil Heat Exchanger ", IJISET - International Journal of Innovative Science, Engineering & Technology, Vol. 2 Issue 8, July.

5. Z. Jianqin and Li Shaopeng, (2014)," Numerical studies an eccentric tube –in –tube helically coiled heat exchanger for IHEP-ADS helium purification system", Institute of High Energy Physics, University of Chinese Academy of science, Beijing,10049, China.

6. R. Kumar, Dr. M. S. Deshmukh, Kamal K. Ghosh, (2015)" Numerical Analysis of Heat Transfer Enhancement in Pipe-in-Pipe Helical Coiled Heat Exchangers ", journal of Mechanical and Civil Engineering (IOSR-JMCE), Volume 12, Issue 6 Ver. II (Nov. - Dec.), PP 70-75.

7. R. Kumar, Kamal K. Ghosh,(2015) " Experimental Study of Heat Transfer Enhancement of Pipe-in-Pipe Helical Coil Heat Exchanger ", journal of Mechanical

and Civil Engineering (IOSR-JMCE), Volume 12, Issue 6 Ver. II, PP 83-86, (Nov. - Dec.).

8. T. P. Golmarz and S. M. Pesteei ,(2012)" Investigation of Dean number and curvature ratio in a double-pipe helical heat exchanger", International Conference on Mechanical Engineering-ISME School of Mechanical Eng., Shiraz University, Shiraz, Iran.

9. G. N., Taherian H., Gorji M.,and Mirgolbabae H., (2010). Experimental study of mixed convection heat transfer in vertical helically coiled tube heat exchangers, Experimental Thermal and Fluid Science, Vol. 34, pp. 900–905.

10. P. Holman, (2002). – Heat Transfer, McGraw Hill Publication, 9th Ed.